Current Journal of Applied Science and Technology

40(2): 1-17, 2021; Article no.CJAST.65528
ISSN: 2457-1024
(Past name: British Journal of Applied Science & Technology, Past ISSN: 2231-0843, NLM ID: 101664541)

Genesis of Meka'a Geophagic Kaolin Deposit (In Foreke-Dschang West Cameroon)

S. A. Douola Ninla[1], G. Kieufack[1], I. Y. Bomeni[2], M. Gountié Dedzo[3] and A. S. L. Wouatong[1*]

[1]Department of Earth Sciences, Faculty of Sciences, University Dschang, P. O. Box 67, Dschang, Cameroon.
[2]Department of Civil Engineering, Fotso Victor University Institute of Technology of Bandjoun, P. O. Box 134, Bandjoun, Cameroon.
[3]Department of Life and Earth Sciences, High Teachers' Training College, University of Maroua, P. O. Box 55, Maroua, Cameroon.

Authors' contributions

This work was carried out in collaboration among all authors. Author SADN conceptualization, investigation, methodology, software, writing and data curation the original draft. Author GK conceptualization, methodology, software and writing the original draft. Author IYB formal analysis data curation software and writing the original draft. Author MGD conceptualization, methodology, software and writing the original draft. Author ASLW visualization, investigation, writing and general supervision the original draft. All authors read and approved the final manuscript.

Article Information

DOI: 10.9734/CJAST/2021/v40i231247
Editor(s):
(1) Dr. Diyuan Li, Central South University, China.
Reviewers:
(1) Bodude Muideen Adebayo, University of Lagos, Akoka, Nigeria.
(2) Yusuf Tanko Usman, Ibrahim Badamasi Babangida University Lapai, Nigeria.
(3) Nasser Y. Mostafa, Suez Canal University, Egypt.
Complete Peer review History: http://www.sdiarticle4.com/review-history/65528

Original Research Article

Received 10 December 2020
Accepted 15 February 2021
Published 05 March 2021

ABSTRACT

Geological, mineralogical and geochemical studies where carried out on Meka'a kaolin deposit located in Foréké-Dschang in order to define the ore genesis. Three kaolin facies (yellow, red and white) and isalteritic components were characterized by different methods including morphostructural description, XRD, XRF, ICP-MS, SEM-EDS, heavy mineral research and organic matter contents. The results show that all these kaolins are based on kaolinite (87–90%) associated with more or less significant phases of orthoclase (1-2%), goethite (0.5-3.5%), quartz (1-1.5%), anatase (1.2-2%) and hematite (1-2%). Small amounts of illite (3.5%) was found only in

**Corresponding author: E-mail: aslwouat@yahoo.com;*

white facies. The scanning electron microscope (SEM) pattern shows that kaolinite particles contained in these kaolins are very small (<2 µm) and are poorly crystallized due to the impurities they contain. Meka'a kaolin's are extremely weathered (CIA and CIW ≈ 100) and their organic matter content is considerable (1.82-2.54%) and is explained by the presence of carbonized wood in the ignimbrites. The combination of different analytical techniques points out a meteoric weathering of ignimbrite under oxidizing conditions as being of petrogenetic origin of this kaolin deposit.

Keywords: Cameroon; clays; hydrothermal alteration; Kaolin; meteoric weathering protolith.

1. INTRODUCTION

Clays are the most utilized industrial minerals in the world and their utilization increases with increase in not of the population [1]. Initially used in craftsmanship as evidenced by the oldest known objects [2, 1], they are nowadays used in various fields including the process industry (beer's filtration; water, wine and oil clarification; [3] and the pharmaceutical industry where they are used as an excipient or active agent for pharmaceutical or cosmetic applications [4, 5] and currently play an important economic role in the world [6]. However, the valorization of clay deposits starts with the mastery of their properties which are conditioned by several factors including mineralogical composition, physical and chemical properties, and the geological condition of formation of these materials [7, 6].

In Africa, Cameroon with his 27 kaolin deposits are one of the african countries with highest number of kaolin deposits recorded [8]. However, more than half of these kaolin deposits have not been characterized [8]. The discovery at the beginning of this century of geophagic clayey materials in the locality of Meka'a (Foreke-Dschang) in Cameroon contributes to the appearance of new kinds of geophagic materials in the local market [9]. Characterization works of these clayey materials have already been initiated by Wouatong et al. [9] and Douola Ninla [10]. They concluded that these materials were much enriched in kaolinite and had both zinc enrichment and some significant heavy metal contents. However, uncertainties persist around the nature of the protolith and the formation of the deposit. In fact, it is known that the Meka'a kaolin deposit is located in a contact zone between pyroclastic products and granito-gneissic basement products [10]. This study seeks to determine the chemical composition and present a mineralogical characterization of the Meka'a kaolin deposit in a bid to understand its genesis and ascertain its quality.

2. NATURAL ENVIRONMENT AND GEOLOGICAL SETTING

The city of Dschang is situated on the Southern flank of mount Bambouto and located at an altitude of 1400 m. Meka'a is a neighborhood of the city of Dschang situated 3 km to the south, between 05°26'05 " and 05°26'33 " North latitude; 10°02'30 " and 10°02'48 " East longitude (Fig. 1).

The Bambouto Mountains is a complex composite polygenic volcanic outfit with an elliptic shape comprised of two caldeiras at its peak. Volcanic activity occurred between 18 and 4.5 Million ago and was at the origin of basic lava flows (effusive type) and much differentiated lavas (extrusive and explosive type) [11]. Basalts, trachytes, phonolites and ignimbrites are the principal products of this active volcano [12]; Fig. 2). These volcanic products directly lay on the granito-gneissic basement and are partially covered in some places by sedimentary and residual formations [13]. The study area is located in a zone covered by volcanic products which are mainly constituted of ignimbritic flows (Fig. 2 and 3). The works of [14, 15] show that Ignimbrites outcrops in Bambouto Mountains are discontinuous and cover approximately 17% (≈ 135 km^2 of the massif with 30 to 120 m in thickness). The volume of these pyroclastic deposits estimated at 13.5 km^3, is actually much larger because these formations are covered by generally lateritized basalts in the southern part of the massif. In the lower zone, they lay on a metamorphic basement, while in the upper zone, they cover trachytic lavas. Welded and non-welded massif lapilli tuff (Tlm) and massif lithic breccias (Brlm) are the two ignimbritic facies cropping out in this massif. The mineralogy of ignimbrites is similar in both massifs; it is made up of quartz, alkali feldspar (sanidine and anorthoclase), plagioclase, biotites and Fe-Ti rich oxides. The lithic fragments are essentially trachytic with proportionately lower rhyolites vitrophyre, fragments of granitic basement,

ignimbrites, scoriae and carbonized woods. Chemical analysis of these rocks indicates a rhyolitic and trachytic composition in mount Bambouto [14, 15].

The granito-gneissic basement in Meka'a is composed dominantly of biotite granite sometimes crossed by granitic veins and containing basic components of orthogneiss [16, 17]). The biotite granite is "intrusive" in the orthogneisses of which it contains blocks in the form of angular spindle-shaped enclaves. On some outcrops, the orthogneiss – biotite granite relationship defines migmatite structures with diffuse granite veins that assimilate orthogneisses or inject into the schistosity plane, thus causing a banding or true gneiss striation. Contact between biotite granite and orthogneisses is fuzzy and often progressive, however granite veins sometimes intersect the outcrops of biotite and amphibole orthogneiss [17]. The biotite granite outcrops in the form of scattered metric balls, near the Foréké chiefdom. It is a heterogranular granite that is fairly homogeneous in its mineralogical composition, within which shreds of orthogneiss, lenses, streaks and clusters of biotite appear [17]. It has a general grainy to grainy porphyroid texture with joined crystals where the feldspar porphyroids appear in a heterogranular grainy matrix composed of quartz, feldspar, biotite and accessory minerals such as titanite, alanite, zircon, iron oxide [17].

Orthogneisses are generally bedded and variable in appearance, both due to the distribution of light beds (quartzo-feldspathic beds) and dark material and to their color. Two petrographic facies have been identified in the Dschang region and defined by [17]. These are biotite and amphibole orthogneisses and biotite orthogneisses. The biotite and amphibole orthogneisses have a granoblastic texture. The clear facies present a "grainy" annealing texture with straight and contiguous grain boundaries. In the dark facies, a relict texture akin to that of tonsillitis dioritis is often observed. It also contains quartz, feldspars and accessory minerals. The dark facies is relatively richer in biotite while in the light facies the proportion of biotite is roughly equal to that of amphibole. Biotite orthogneisses are light to dark grey with medium to fine grain. They are sometimes found in small slabs or bands, of two to three meters

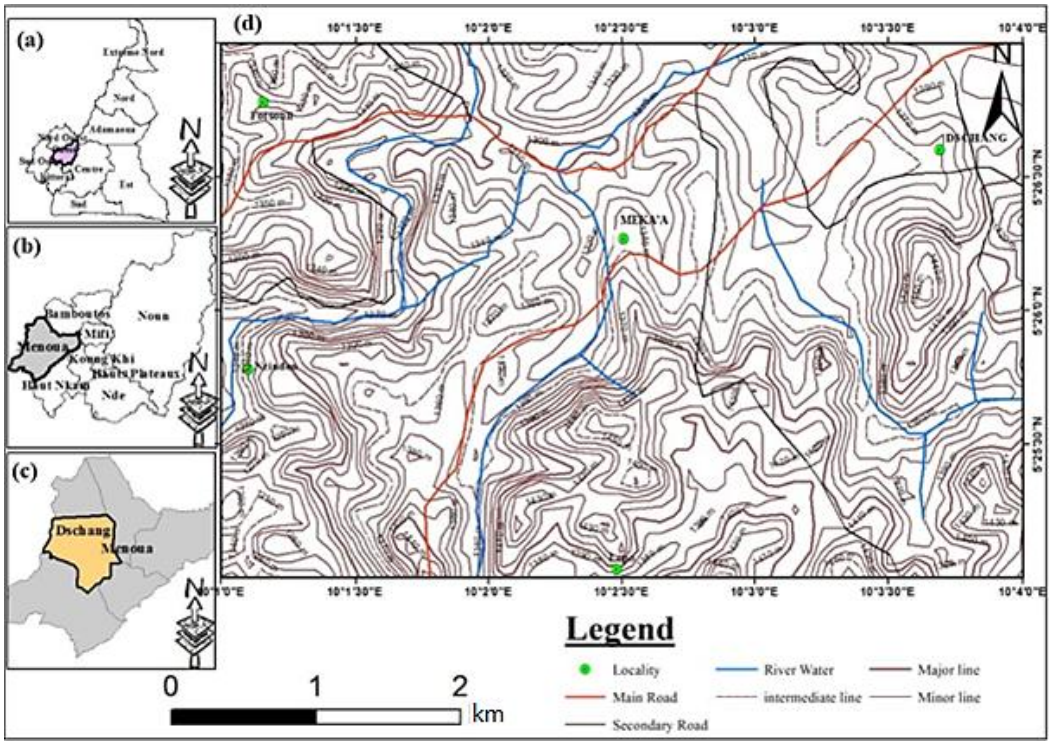

Fig. 1. Location map: The Western Region in Cameroon (a); the Department of Menoua in the Western Region (b); the city of Dschang in the Department of Menoua (c); the site of Meka'a (d). (extracted from the Bafoussam 1C - 1/50.000 map)

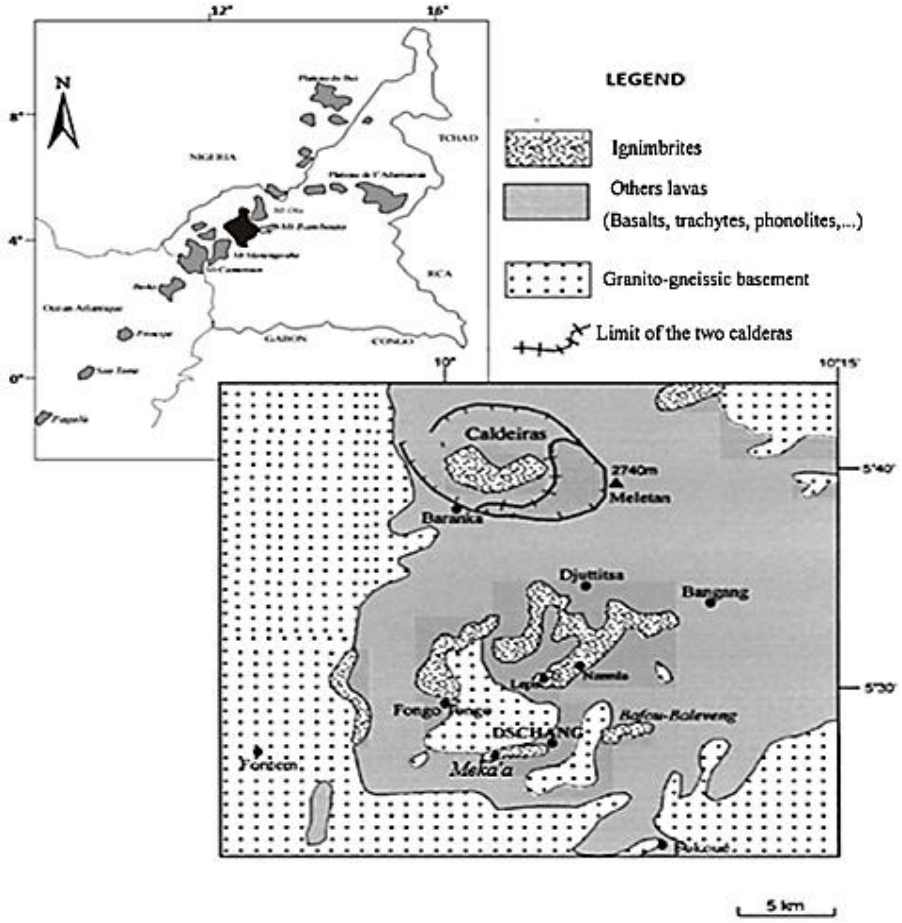

Fig. 2. Location of the Bambouto Mountains in the Cameroon Line and indications on the distribution of ignimbritic deposits and lava [12]

thick interspersed between outcrops of biotite and amphibole orthogneiss. From a cartographic point of view, they emerge between biotite granites and biotite and amphibole orthogneisses. They are also found in septa form in biotite granites. They are finely bedded and their schistosity is more pronounced on the outcrop and under the microscope than on the sample scale. The biotite orthogneisses are essentially granoblastic in texture with medium to fine grain. Biotite orthogneisses are also composed of quartz, alkali feldspar, plagioclase and titanite [17].

3. METHODOLOGY

3.1 Fields Works

After a preliminary reconnaissance survey, ten trial pits were dug manually (using a pickaxe, crowbar, machete, shovel, etc.) to observe the morpho-structural organization of the area and to collect samples of clayey materials, for laboratory analysis. Depending on the similarities observed on these trial pits profiles, three representative trial pits was chosen for the description. The description of the profiles of the representative trial pits was made along the walls of the latter. This description made it possible to identify the different homogeneous layers (horizons) that make up these profiles. Coloration was determined using the Munsell soil color chart. Texture, structure and compactness was determined using in situ techniques (sausage test, arrangement of soil particles, knife penetration).

Eight soils samples were taken from the walls of the trial pits and placed in polythene bags which were sealed and labeled. These samples were then air dried and reduced to powder for further laboratory analysis.

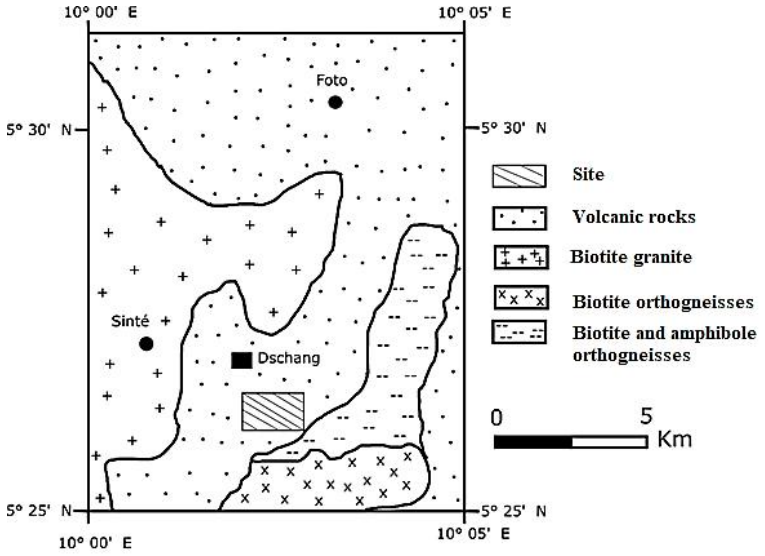

Fig. 3. Geological map of the Dschang region (after Kwekam et al. [17])

3.2 Experimental Procedures

3.2.1 Mineralogical analysis

Determination of the mineralogical composition of the samples was made using X-ray diffractometry. It was carried out in two stages. Firstly, on the aggregate sample and then on the clay fraction.

The total mineralogy was carried out using the Brucker D8-Eco diffractometer using the Kα1 radiation of copper (λ = 1.54Å) in the laboratory Research Unit of Clays and Sedimentary Environment (URAGEs) at the University of Liège. Samples have been treated in order to limit the preferential orientation of the minerals according to the method of Moore and Reynolds (1989) before being introduced into the diffractometer whose X-ray scanning angle is between 2 ° and 70 ° 2 θ.

The mineralogy of the clay fraction requires three diffractions (normal diffraction, ethylene glycol diffraction, and diffraction on heating at 500°C) with a scanning angle between 2° and 30° 2θ. Samples was treated here with ethylene-glycol and heated to 500°C before being subjected to X-ray diffraction. Using EVA software, was then used to superimpose diffractograms in order to identify the different groups of clay minerals contained in the sample.

The mineralogical composition was calculated using the method of [18]. To do this, SiO_2, Al_2O_3 and K_2O are taken for clay minerals and identified feldspars, TiO_2 is taken for anatase, excess silica is taken for quartz and Fe_2O_3 is taken for the iron oxy-hydroxides identified. The difference between the mass percentages provided by the chemical analysis data and those of all identified minerals is taken to define the undetermined.

3.2.2 Physico-chemical analysis

3.2.2.1 Organic Matter

The organic matter content (T_{MO}) was determined according to the protocol summarized below. In order to determine organic matter content, samples were crushed and then dried in an oven at 105°C during 24 h. The mass of the dry sample (M_a) was determined using an electronic balance to the nearest 1/1000. Then, the samples were placed in the porcelain micro crucibles and calcined at 550°C for 4 h in an electric oven [19]. After cooling in the oven, the mass of the calcined sample (M_b) was determined and the level of organic matter as given by formula. The organic matter was assayed in the laboratory of the Local Materials Promotion Authority (MIPROMALO).

$$T_{Mo} = \frac{(M_a - M_b)\times 100}{M_a} \quad (1)$$

3.2.2.2 Geochemical analysis

The geochemical analyses mainly concerned the determination of major elements by X-ray

fluorescence (XRF) and rare earths elements by Inductively Coupled Plasma Mass Spectrometry (ICP-MS). All these analyses were carried out in the Mineralogy Laboratory of the University of Liège.

For XRF, samples previously dried in an oven at 105°C, calcinated, crushed and then molten after being mixed with Lithium metaborate. The liquid resulting from the fusion was poured into a mold which, after cooling, releases the bead and that was ready for spectrometer analysis and the result was given in oxide percentage. Thermo Fischer Niton XL3D GOLD apparatus was used.

ICP-MS was performed after melting 1g of each sample mixed with approximately 3g of lithium metaborate ($LiBO_2$) in a tunnel oven at 980°C for 1 hour. The mixture was then dissolved in the solution of nitric acid (1.55M), then stirred in polypropylene container for 12 hours at a temperature of 20°C before analysis by the Agilent 7500 type apparatus. The results were given in ppm.

3.2.3 Microscopic observations

3.2.3.1 Scanning Electron Microscopy and Energy Dispersive Spectrometry

These observations were made on the FEG-ESEM XL3 device at the chemistry laboratory of the University of Liège. Images were obtained by secondary electron detector after powder metallization with gold by plasma spraying (distance 5 cm, 30 mA, 0.05 atm of argon, 50 seconds). The acceleration voltage is shown in the taken pictures (10.0 kV and 15.0 kV). The images were taken at different magnifications (600 ηm; 1; 3 and 5 µm) according to the texture identified on these clays. The local chemical analysis was determined by combining SEM with the energy dispersive spectrometer.

3.2.3.2 Heavy minerals observations

Heavy minerals are those with a specific gravity greater than 2.89. Their analysis was carried out at the Institute of Geological and Mining Research in Cameroon. Only isalteritic products were concerned in this study. Two isalteritic samples (DM24 and DM28) were concerned with the search for heavy minerals. The sample DM28 was separated into two phases (a and b) according to the two main phases of this horizon. Techniques used for sampling, the extraction and the mounting of heavy minerals on slides during this study were those recommended by [20] and [21].

4. RESULTS

4.1 Morpho-Structural Organization of Weathering Profile of Meka'a

Three representative trial pits were described. The first trial pitt show an organization of two main horizons, BC and C (with five different level) (Fig. 4). From the surface to the base, we have:

- A polyphasic horizon BC (0-260 cm) with a yellow clayey matrix (2.5Y 7/6). This matrix has a fragmented structure and contains many white micrometric punctuations of about 1.5 to 4 cm diameter. This horizon has probably been highly disturbed during road works;
- A pale yellow (2.5Y 8/4) clayey level C1 (260-370 cm) with a massive structure;
- A pale red clayey C2 level (370-570 cm) with a massive structure;
- A yellow (2.5Y 7/8) silty clayey isaltéritic C3 level (570 -825 cm) with many white inclusions;
- A polyphasic clayey C4 level (825-1025 cm). Pale yellow (2.5Y 7/4), clear brown (7.5YR 6/4) and pale red (7.5R 6/4) are the three phases identified in this horizon. yellow and red phases have a massive melted structure and only the brown phase shows micrometric whitish punctuations;
- A compact yellow silty clayey isalteritic C5 level (1025-1500 cm) with many white particles.

Level C1 and C2 contain edible clayey materials which correspond to the kaolin sold in the market. The real geophagic soils deposit was found as from the depth of 850 cm to 1025 cm (Level C4). Macroscopically, these layers were presented as a thicker superposition of levels C1 and C2. The C5 level has a yellowish matrix laced with whitish inclusions of various sizes and shapes. These facies are similar in all respects to that of ignimbrite altered in the Dschang region as described by [22] and [12]. These ignimbrites have actually a massive lapilli tuff facies (Tlm) marked by the presence of ovoid lenticular fiames (5 to 10% of the rock), rock fragments (especially trachytic) and finally a glass matrix [12, 23] index possible ignimbritic origin of these materials. However, no mineral relic can be identified with the naked eye, as this reflects a very intensive degree of weathering. It is

important to note here that the C5 level is comparable to a thicker C3 level.

In addition to the above-mentioned horizons, the trial pit two shows the presence of:

- an A horizon (organo mineral horizon) with low thickness;
- an additional whitish clayey phase (10YR 8/1) in the C4 level; the limits between these three clayey phases are very diffuse here (Fig. 4);
- an C6 level with grey color more compact than C5 level and still similar in appearance to pyroclastic materials undergoing the weathering process according to their lithic structure and silty-clayey texture (Fig. 4).

In the trial pit three, the C5 level is not very thick (about 100 cm) and rests directly on a C7 level a few centimeters thick. Level C7 is made exclusively of hard material and has a lamellar structure. The C7 level is based on a multi-phase C8 level (red and white) with a sandy clayey texture and a lithic structure. But here, the C8 level is closer to a grainy rock's weathering product (Fig. 4).

4.2 Research and Heavy Minerals Identification in Isalteritic Materials

The heavy minerals identified were zircon, tourmaline, garnet, chloritoids, anatase, zoisite, diopside, and opaque minerals. Opaque minerals are the most abundant (60-95%). The DM24 sample in addition to the opaque minerals only contains garnet (6%), anatase (2%) and tourmaline (2%). Sample DM28a is devoid of zircon and has the lowest level of opaque minerals (60%) but has the highest number of other minerals. Sample DM28b is the only sample with zircon and displays the highest number of opaque minerals. The heavy minerals found was shown in Fig. 5.

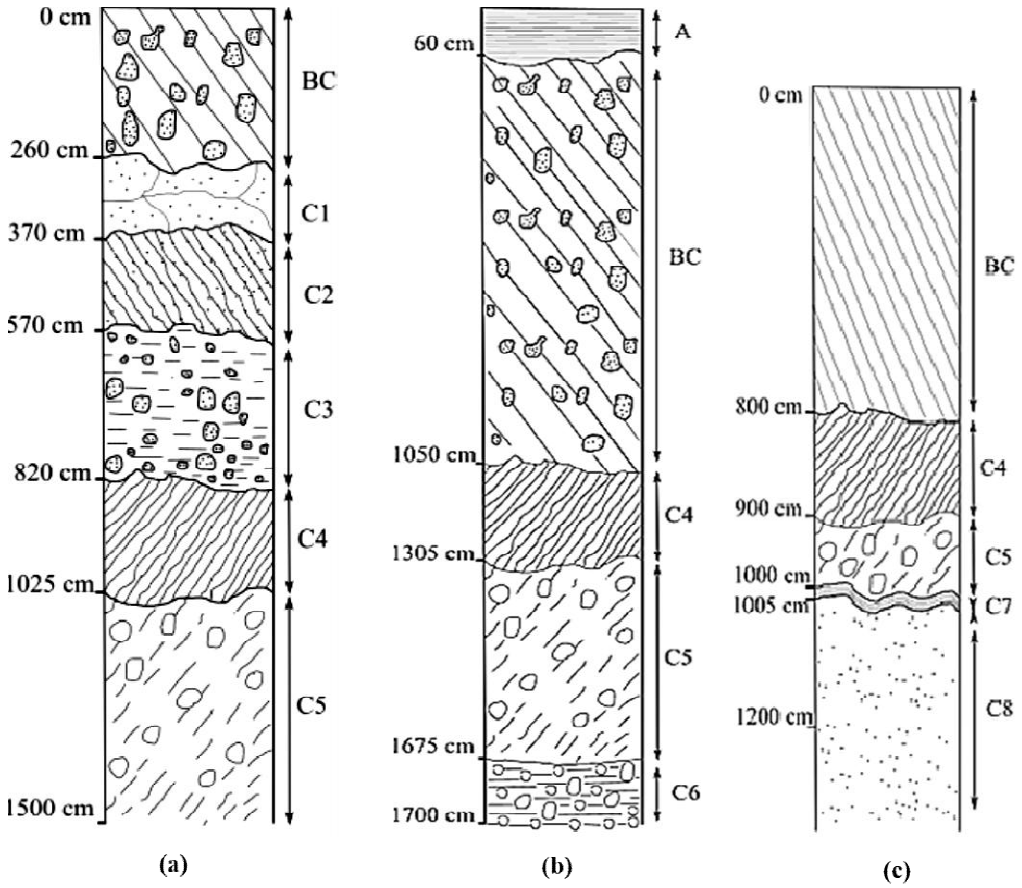

Fig. 4. Morpho-structural sections of the trial pits. (a): trial pit 1 profile; (b): trial pit 2 profile; (c): trial pit 3 profile

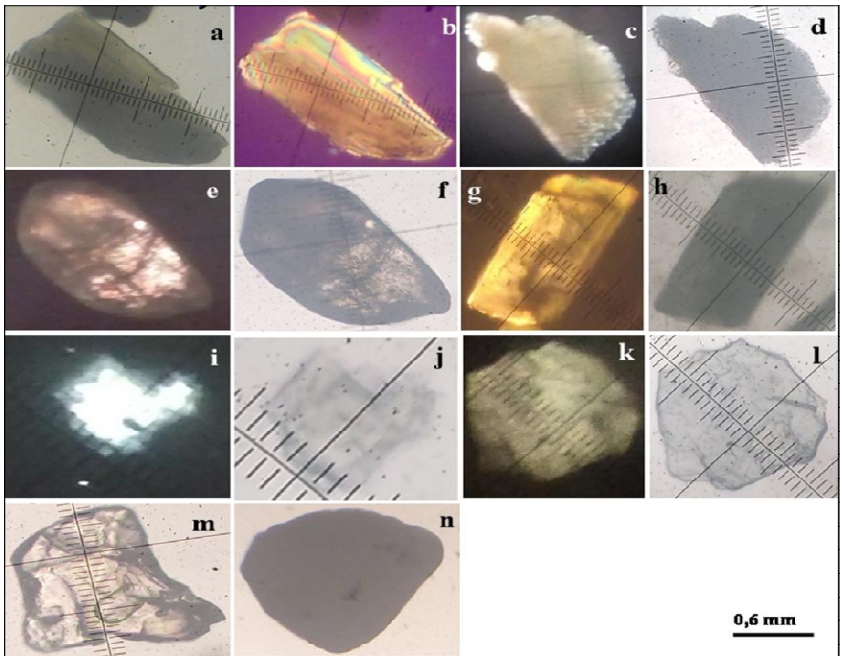

Fig. 5. Identified heavy minerals in isalteritic products of the Meka'a profile. a) Diopside LPNA b) Diopside LPA; c) Anatase LPA d) Anatase LPNA, e) Zircon LPA; f) Zircon LPNA, g) Tourmaline LPA; h) Tourmaline LPNA, i) Zoisite; j) Zoisite LPNA; k) LPNA chloritoid; l); LPA chloritoid, m) Garnet, n) Opaque mineral

4.3 Organic Matter Content in the Kaolin of Meka'a

As shown in Table 1, the organic matter content of the kaolin of Meka'a are considerable (≥2%).

Table 1. Organic matter content of the Meka'a kaolin deposit

Samples	% OM
DM15	2,16
DM16	2,23
DM17	2,54

4.4 Mineralogical Profile of the Clayey Materials of Meka'a

The powder diffraction pattern of the clay materials (DM15, DM16 and DM17) indicate the dominant presence of kaolinite associated with phases of goethite, hematite, anatase and quartz in all these samples. The isalteritic materials also display a similar composition, but with more pronounced quartz peaks, especially in sample DM28 (Fig. 6). The sample DM 25 (indurated material) show, in addition to the phases mentioned above, an imposing peak of gibbsite (Fig. 6). The mineralogical quantification of these materials indicates on one hand that the clayey materials (DM15, DM16 and DM17) are based of kaolinite (≈90%) associated minor phases of orthosis (1- 2%), goethite (0.5-3.5%), quartz (1-1.5%), anatase (1-2%) and hematite (1-2%). Illite is present in very low proportions (3.5%) in sample DM17. On the other hand, the other materials in the profile, namely, ignimbritic isalterite (DM24) and granito-gnessic basement isalterite (DM28) are all also made up of kaolinite (89 and 78% respectively) associated with orthosis (1-2%), goethite (1 and 4% respectively), quartz (1.5 4% respectively), anatase (1.5 and 1% respectively) and traces of hematite (1%). Sample DM28 additionally contains 12% illite. The hardened material has a very different composition. Kaolinite, quartz and gibbsite (7, 5 and 80% respectively) are the dominant components followed by hematite (3%), orthosis (2%), goethite (1%) and anatase (0.5%). Overall, the proportion of undetermined varies from 1 to 3% and may be due to the simplification of reconstitution scheme.

The photomicrographs obtained from SEM shows clusters of pseudo-hexagonal particles of poorly crystallized kaolinite embedded in a silico-aluminous gel and abundant micropores. The clusters of poorly crystallized kaolinite particle

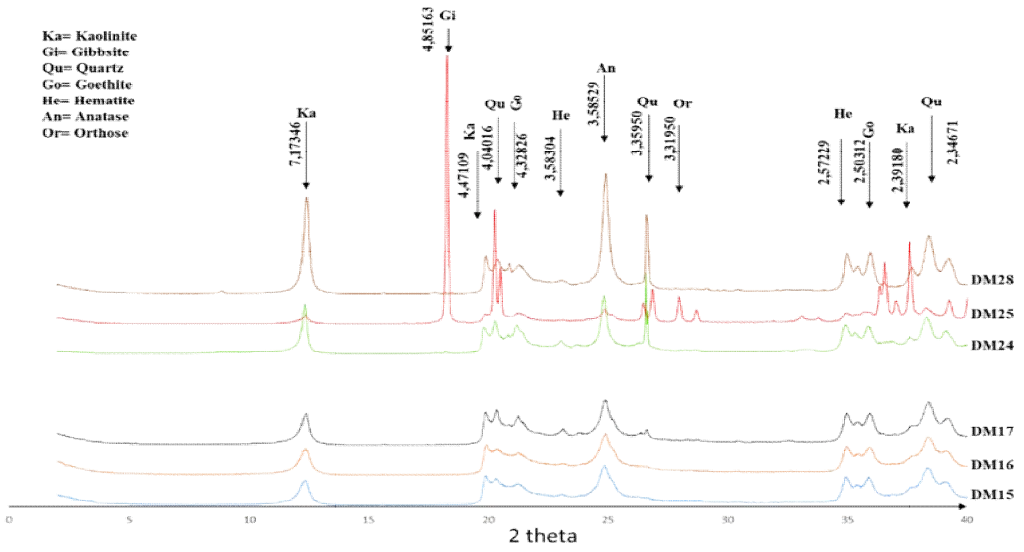

Fig. 6. Samples XRD patterns

are stacked in disorder. Kaolinite particles are very small (<1 µm) and generally irregular in shape (Fig. 7). EDS spectral analysis (Fig. 7) indicates a dominance of aluminum and silicon with fairly close peaks in these clay materials. This is characteristic of kaolinite mineral.

4.5 Geochemistry

SiO_2 is the most abundant element in these samples, followed by Al_2O_3. MnO, MgO, Na_2O and CaO have almost zero levels in all of these samples. More specifically, the samples of clay materials have SiO_2 contents close to 40%. Al_2O_3 has levels of between 28.71% (DM16) and 37.79% (DM22). Fe_2O_3 is the third most abundant oxide in these products, and its contents range from 1.65% (DM17) to 1.96% (DM15). TiO_2 for its part has contents varying from 1.25% (DM 16) to 1.65% (DM17). K_2O, Na_2O and P_2O_5 have contents lower than 0.1%. MgO and CaO show contents close to 0.1%. The MnO contents are almost zero (0.01%). The loss on ignition varies from 13 to 17%. The SiO_2/Al_2O_3 molar ratio is close to 2, which marks the dominance of type 1:1 minerals like kaolinite.

Isalteritic samples and indurated materials shows almost the same trend. SiO_2 dominates in samples DM24 and DM28 (43.34 - 48.07% respectively) while in sample DM 25 it is in the minority (9.72%) ahead of Al_2O_3 (56.47%). The Al_2O_3 content in samples DM24 and DM 28 is around 35%. The Fe_2O_3 content varies in these isalterites from 1% (DM28) to 6% (DM24). The alkali and alkaline earth contents are very low (<0.2%). The ignition loss is high in sample DM25 (28.8%).

Chemical index of Alteration [24] and Chemical index of weathering [25] were calculated using formulas (2) and (3) bellow.

$$\mathrm{CIA} = \frac{\mathrm{AL_2O_3}}{(\mathrm{AL_2O_3} + CaO + Na_2O + K_2O)} \times 100 \quad (2)$$

$$\mathrm{CIW} = \frac{\mathrm{AL_2O_3}}{(\mathrm{AL_2O_3} + CaO + Na_2O)} \times 100 \quad (3)$$

Where Al_2O_3, K_2O, Na_2O and CaO represent the percentages of theses oxydes obtained from chemical analyse of samples. Calculations gives values close to 100 for all these samples.

The values obtained for the rare earth element (REE) range from 1.33 to 446 ppm in clay materials and 0.33 to 666 ppm for the other samples. The ratio of light rare earth element by the heavy rare earth element (LREE/HREE) is particularly very high in the DM28 sample (Table 2). The REE patterns of isalteritic materials normalized to C1 chondrite [26], show positive Cerium (Ce) and negative Europium (Eu) anomalies. When these samples are normalized to the Kemtswop IBT2 ignimbrite matrix from the work of [27], the curves look the same except the disappearance of negative Eu anomaly (Fig. 8). It is important to note that curves of ignimbritic isalterite and indurated material are almost identical and parrallel.

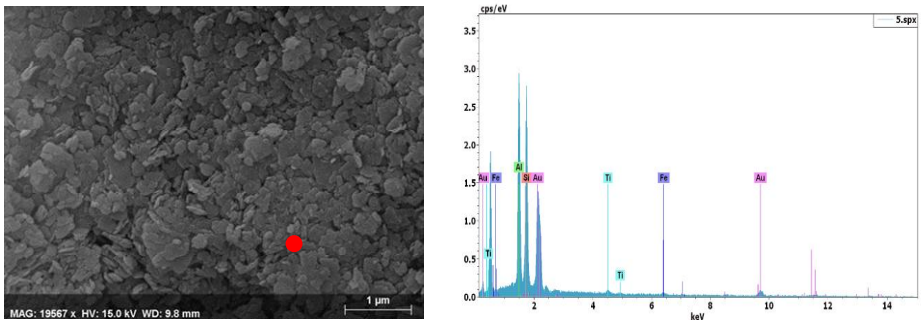

DM 15

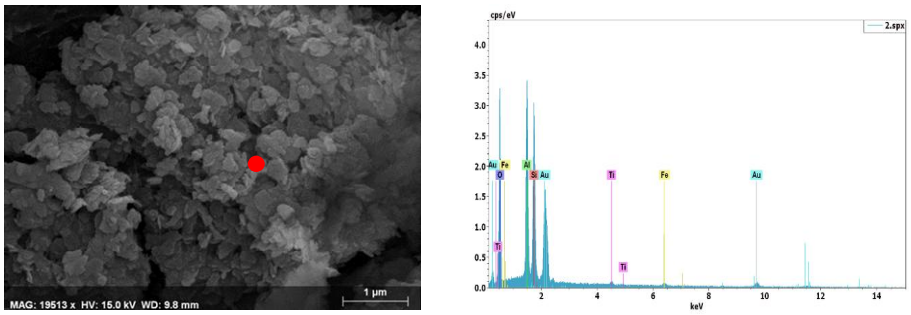

DM 16

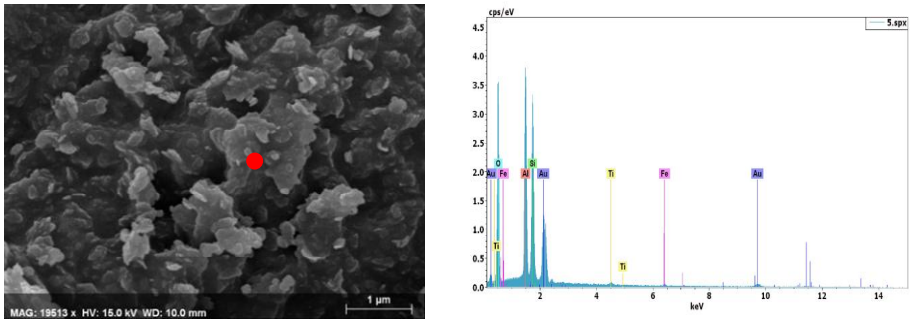

DM 17

Fig. 7. SEM microphotographs and EDS spectra

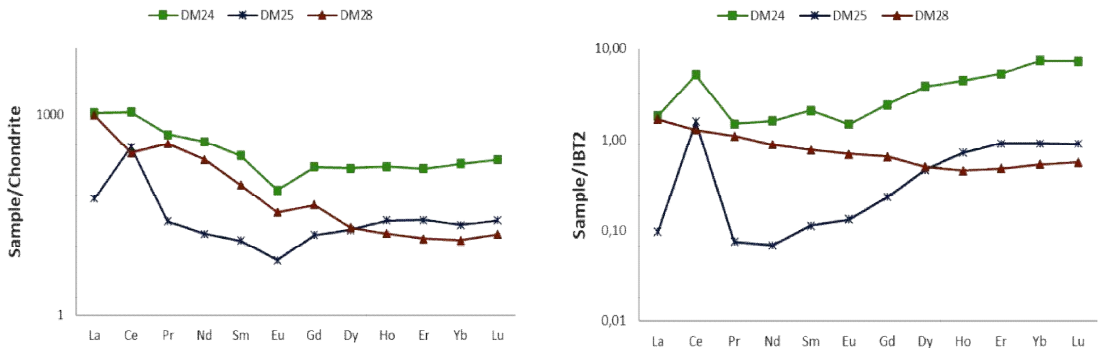

Fig. 8. REE contents of Meka'a isalteritic materials normalized to Chondrite C1 and Ignimbrite matrix IBT2

Table 2. Major elements and REE composition of kaolin and isalteritic materials from Meka'a deposit

Samples	Kaolin samples			Isalterite samples		
	DM15	DM16	DM17	DM24	DM25	DM28
Major elements (%)						
SiO_2	36.05	34.30	44.89	43.34	9.72	48.07
TiO_2	1.30	1.20	1.65	0.42	0.75	0.57
Al_2O_3	30.12	28.71	36.53	34.44	56.47	36.07
Fe_2O_3	1.96	1.74	1.65	6.44	4.10	1.00
MnO	0.01	0.01	0.02	0.10	0.01	0.01
MgO	0.08	0.06	0.11	0.11	0.12	0.09
CaO	0.06	0.06	0.07	0.09	0.05	0.08
Na_2O	0.11	0.07	0.06	0.07	0.07	0.07
K_2O	0.04	0.04	0.06	0.01	0.00	0.28
P_2O_5	0.06	0.06	0.09	0.15	0.03	0.05
LOI	1.30	15.43	16.03	16.17	28.80	13.92
∑	8.09	81.68	101.16	101.34	100.12	100.21
SiO_2/Al_2O_3	2.03	2.03	2.09	2.14	0.29	2.27
CIA	99.31	99.41	99.48	99.51	99.79	98.82
CIW	99.44	99.55	99.65	99.54	99.79	99.59
Rare earth elements (ppm)						
La	259	291	446	250	13	231
Ce	151	153	273	666	202	163
Pr	32	37	66	47	2	34
Nd	81	93	173	180	8	98
Sm	12.5	13.2	24	36	2	13
Eu	2.3	2.5	3.8	4	0	2
Gd	9.7	10.3	17.7	33	3	9
Dy	9.6	9.8	18.0	39	5	5
Ho	2.1	2.1	3.8	8	1	1
Er	6.1	6.1	11.1	25	4	2
Yb	6.7	6.8	12.3	30	4	2
Lu	0.98	1.00	1.83	4	1	0
∑REE	573.2	625.7	1050.4	1323.28	245.48	561.38
LREE/HREE	15.3	16.3	15.2	8.48	12.94	27.77

5. DISCUSSION

5.1 Nature of the Protolith

The C3, C5 and C6 isalteritic levels, by the arrangement of their components are similar to ignimbritic products of the Dschang region as described by [28, 22], [12]. This idea is further reinforced by the location of this site near the Dschang-Fossong-Wentcheng road cut known to harbor ignimbritic formations [28, 22, 29], and quite close to the Zideng and Kemtswop sites which provided ignimbrite samples for the work of [27].

The first trial pit clearly shows a repeating sequence of the deposit of clay ore based on an ignimbritic isalterite. Firstly C1 and C2 levels (containing geophagic clayey materials) resting on the C3 level (ignimbritic isalterite). Secondly, the C4 level (main deposit) rest on the ignimbritic alterite (levels C5 and C6) (Fig. 4). This suggests two thin phases of pyroclastic deposits, with the C4 level having been presented already as a thicker distribution of the C1 and C2 levels [10].

Moreover, the profile of the third trial pit (Fig. 4) shows, at its base, the alteration product of an coarse grained rock similar to sandy arena not far exploited for the production of sand. It is therefore possible that we are here in the presence of an alteration profile of ignimbritic materials resting on the alteration product of the granito-gneissic basement. A thinny indurated level separates these two units and indicates an aborted bauxitization process. This arrangement of weathering products of an ignimbritic nature based on weathering products of the granito gneissic basement corresponds perfectly to the presentation of ignimbritic flows in this part of the

Bambouto volcano as presented by [28, 22, 12]; 15, 27, 30].

The heavy minerals contents also help to identify the protolith on the one hand and garnet, tourmaline, anatase and opaque minerals are found both within volcanic and metamorphic rocks; zoisite and chloritoid are reputed to be indicators of regional metamorphism and hydrothermal alteration [31]. On the other hand, diopside is commonly present in volcanic ultramafic and metamorphic rocks. Biotite granite; biotite orthogneiss and biotite and amphibole orthogneiss from Dschang region contain zircon as accessory mineral [17]. Thus, the presence of zircon, diopside, zoisite, and chloritoid only in samples DM28 (a) and (b) from the C8 level shows that this level is an alteration product of the granito-gneissic basement. In turn, sample DM24 (horizon C5) is lacking in these heavy minerals which come from another source rock.

Geochemically, the europium anomaly (Eu) and the LREE/HREE ratio can be viewed as indicators of the source rock [32]. A high LREE/HREE ratio associated with a negative Eu anomaly is generally observed in felsic rocks while mafic rocks most often exhibit a low LREE/HREE ratio with little or no Eu anomaly at all [33, 34]. TTG (Tonalite-Tronjhemite-Gneiss) rocks exhibit a very high LREE/HREE ratio with little or no Eu positive anomaly [35]. In the present case; all samples normalized to Chondrite C1 show high LREE/HREE ratio (9-16) and a negative Europium abnormality. The source rock in this case should be sought-after within felsic rocks. This is normally suitable to the ignimbrites from the Dschang region which have been reported to have a rhyolitic composition [28, 22, 12, 14, 15, 27] and are included among the felsic lavas from Bambouto Mountain [27].

REE pattern normalized to Chondrite C1 and IBT2 ignimbrite confirm, on the one hand by their parallel and stacked shapes that sample DM24 (isalteritic ignimbritic material) and sample DM25 (indurated material) derive from the same source rock and have undergone the same weathering process. The composition of their source rock in this case are closer to those of IBT2 ignimbrite matrix. On the other hand, the divergence recorded between these spectra with the spectrum of sample DM28 confirms that these weathering products are derived from two different source rocks.

In the final analysis, considering the depth of sampling (around 10 m), the high level of organic matter (≥2%) present in these clay materials can only be explained by the presence of carbonized wood in the ignimbrites during their placement. This presence of carbonized wood within ignimbrites is well known and described in the Dschang region by [15].

5.2 Weathering Processes

Two alteration modes can be considered at this level. Hydrothermal alteration and meteoric weathering. While it is easy to establish the hydrothermal origin of the high temperature facies, it becomes more difficult when the temperature drops considerably [36]. Indeed, a strong resemblance (mineralogical and geochemical) is established between hydrothermal alteration at low temperature and meteoric alteration [36]. The mineralogical phases common to these forms of weathering are smectite, vermiculite, kaolinite and illite [37]. However, the geological context of the site, the morphostructural organization of the deposit, the associated mineral phases and the geochemical data are important clues used to differentiate these two alteration modes [38, 39, 40].

In Meka'a, the presence of the granito-gneissic bedrock containing intrusions as described by [16, 17, 30] would promote the circulation of hydrothermal fluids. Likewise the intense volcanic activity (marked by a succession of pyroclastic deposits on the site) would greatly contribute to the hydrothermal alteration process [41, 42, 43, 44]. However, the ferralitic character observed on the different trial pits by analogy with the alteration product around the mylonitic bands of Mayouom [37] supports the thesis of a meteoric alteration [45].
On this momentum, mineralogical analysis indicated the association of kaolinite, quartz, goethite, hematite and anatase as mineral phases present in these materials. This sub-surface mineralogical assemblage is quite different from those reported by several authors as products of hydrothermal alteration [46-49, 40, 50, 51, 37]. In addition, the low content or absence of relic minerals (quartz, micas, orthosis, etc.) in these materials also argues against a hydrothermal origin [52, 53]. Likewise, the complete absence of minerals indicative of hydrothermal alteration such as florencite, pyrite, chrysotile and lizardite in the paragenesis of Meka'a clay materials totally eliminates the idea of hydrothermal alteration [45, 54, 37, 55]. Finally, it is known that in a tropical climate, meteoric weathering favors the presence of iron

oxides and hydroxides in weathering products [38, 56] as is the present case with the Meka'a materials which have significant phases of goethite [FeO (OH)] and hematite (Fe_2O_3).

The EDS spectra of these clayey materials show impurities cations (Fe, Ti…) whose abundance in the materials are at the origin of the poor crystallinity of kaolinite and the small size of their particles [57]. This poor crystallinity is an indicator of the meteoric weathering in a humid tropical climate which led to the formation of this product [45, 58, 54, 37]. Likewise, the abundance of pores in these materials indicates that these kaolinite minerals were formed during meteoric weathering [59].

Hydrothermal kaolin deposits are known to be rich in phosphorus and sulfur (because of the pyrite they contain) and in phosphate and sulphated aluminum minerals [37]. Also, the low content of P_2O_5 and the total absence of SO_2 corroborate the thesis of a meteoric weathering having preceded the formation of the deposit of clayey materials of Meka'a [38, 39]. Likewise, the low contents obtained for TiO_2 argue against hydrothermal alteration. The presence of anatase (in small quantities) can be considered as the product of the precipitation of oxides during the weathering of titanium or ferrotitanium primary minerals [60, 61].

The positive or negative anomalies recorded for Ce argue against a hydrothermal alteration which is generally marked by an absence of Ce anomaly. Positive Cerium anomalies occur when Ce^{3+} has been oxidized to Ce^{4+} in an oxidizing environment [47, 45, 54, 62, 47, 63, 64]. They can also be explained by the subsequent formation of CeO_2 [65]. During weathering, Ce may indeed have rapidly precipitated in the form of cerianite (not detected by the mineralogical analysis here) as is the case for the alteration of granites from Sulawesi Island in Indonesia [66] and for the lateritic profiles of Goyoum in the Eastern Region of Cameroon [45].

According to the work of [67], Eu anomalies index hydrothermal origin of REE and their absence is generally associated with low temperature alteration. The absence of an anomaly with Eu in the samples normalized to the ignimbrite matrix shows in this case that the reaction environment during the weathering process was not reducing as is the case during hydrothermal processes during which Eu^{3+} is reduced to Eu^{2+} [68]. Negative Eu anomalies are often associated with the presence of slightly altered feldspars which trap this element [69] and their absence in the present case can be assimilated to a weak presence of unweathered feldspars.

6. CONCLUSION

The Meka'a kaolin deposit presents a superposition of ignimbrite weathering products resting on weathering products of the granito-gneissic basement and from which they are separated by an induration zone, thus reflecting an aborted bauxitization process. These kaolins present three facies; yellow, red and white. The mineral assemblage mainly comprises alumina silicates (mainly kaolinite) and iron oxyhydroxides. The kaolinite particles are very small in size and are poorly crystallized and these materials are rich in pores. The presence of Ce anomalies and the absence of Eu anomalies indicate the oxidative nature of weathering conditions. All of these characteristics lead us to believe that the Meka'a kaolin deposit comes from the meteoric weathering of ignimbrite. However, according to the geological context marked by the presence of the metamorphic formations, a slight hydrothermal influence during weathering could have taken place.

COMPETING INTERESTS

Authors have declared that no competing interests exist.

REFERENCES

1. Nkoumbou C, Njoya A, Njopwouo D, Et Wandji R. Intérêt économique des matériaux argileux. Actes de la première conférence sur la valorisation des matériaux argileux au Cameroun et de la création du groupe camerounais des argiles. Yaoundé, Avril, French. 2001; 11-12.
2. Gamble. The paleolithic settlement of Europe. Cambridge university press; 1986.
3. Caillere S, Henin S, Rautureau M. Les argiles. *Ed.* Septima, Paris; 1989.
4. Carretero MI. Clay minerals and their beneficial effects upon human health. A review. Appl. Clay Sci. 2002;21:155–63.
5. Carretero MI, Gomes C, Tateo F. Clays and human health. In: Bergaya F, Theng

BKG, Lagaly G. (Eds.), Handbook of Clay Science. Elsevier, Amsterdam;
6. Murray HH. Traditional and new applications for kaolin, smectite, and palygorskite: A general overview. App. Clay Sci. 2000; 17(5):207-221.
7. Murray HH, Keller WD. Kaolin, kaolin and kaolin. In: Murray HH, Bondy W, Harvey C (Eds.), kaolin genesis and utilization. Special Publ. The Clay Miner. Soci. 1993; 1:1–24.
8. Ekosse GI E. Kaolin deposits and occurrences in Africa: Geology, mineralogy, and utilization. Applied Clay Science. 2010; 50:212–36.
9. Wouatong ASL, Douola Ninla SA, Yongue Fouateu R, Tématio P, Njopwouo D. Etude géologique et caractérisation minéralogique et chimique des argiles de Meka'a (Foréké-Daschang; Ouest-Cameroun). Actes Conférence sur les matériaux argileux d'Afrique Centrale. Yaoundé, French. 2008; 19-22.
10. Douola Ninla SA, Wouatong ASL, Tchounang Kouonang S, Yerima B, Njopwouo D. Mineralogical and physico-chemical characterization of clayey materials of meka'a (West Cameroon) Preliminary Step for Their Utilization for Human Ingestion, Earth Sciences. 2018; 7(5):74-85.
11. Nni J. Et Nyobe JB. Géologie et pétrologie des laves précaldériques des monts Bambouto: Ligne du Cameroun. Geochemica Brasiliensis. 1995; 9(1):47-59.
12. Nono A, Njonfang E, Kagou Dongmo A, Nkouathio D, Tchoua FM. Pyroclatic deposits of the Bambouto volcano (Cameroon Line, Central Africa): Evidence of a strombolian initial phase. Journ. African Earth Sci. 2004; 409-14.
13. Youmen D. Evolution Volcanique. Pétrographique Et temporelle de la caldeira des months Bambouto (Cameroun). Thèse doc. Univ. Kiel, Allemagne, French; 1994.
14. Gountie Dedzo M, Nono A, Njonfang E, Kamgang P, Zangmo Tefogoum G, Kagou Dongmo. Le volcanisme ignimbritique des monts Bambouto et Bamenda (Ligne du Cameroun, Afrique Centrale) : signification dans la genèse des caldeiras. Bulletin de l'Institut Scientifique, Rabat, Section Sciences de la Terre. 2011; 33:1-15.
15. Gountié Dedzo M, Njonfang E, Nono A, Kamgang P, Zangmo Tefogoum G, Kagou Dongmo A, Nkouathio DG. Dynamic and evolution of the Mounts Bamboutos and Bamenda calderas by study of ignimbritic deposits (West-Cameroon, Cameroon Line). Syllabus Review, Sci. Ser. 2012; 3:11–23.
16. Bouyo Houketchang M. Etude tectonique et métamorphique de la région de Dschang (Ouest Cameroun). Mém DEA. Univ. Yaoundé I, French; 2003.
17. Kwékam M. Genèse et évolution des granitoïdes calco-alcalins au cours de la tectonique panafricaine ; Le cas des massifs syn à tardi tectonique de l'Ouest Cameroun (Région de Dschang et de Kékem. Thèse Doct. d'Etat, université de Yaoundé, French. 2005; 1.
18. Njopwouo D. Minéralogie de la fraction fine des argiles de Bomkoul et de Balengou (Cameroun). Utilisation dans la polymérisation du styrène et dans le renforcement du caoutchouc naturel. Thèse Doct. d'Etat Univ. Yaoundé I. French; 1984.
19. Heiri O, Lotter AF, Lemcke G. Loss on ignition as a method for estimating organic and carbonate content in sediments: reproducibility and comparability of results. Journal of Paleolimnology. 2001;25:101-10.
20. Duplaix S. Détermination microscopique des minéraux de sables. Librairie Polytechnique C. Béranger, Paris. French; 1958.
21. Parfenoff A, Pomerol C, Tourenq J. Les minéraux en grains. Méthodes d'étude et détermination. Eds Masson, French; 1970.
22. Tchoua FM. Sur l'existence d'une phase initiale ignimbritique dans le volcanisme des monts Bambouto (Cameroun). Comptes Rendus de l'Academie des Sciences Paris, French. 1973; 276:2863–66.
23. Poueme Djueyep G. Caractérisation minéralogique et géotechnique des matériaux d'altération développés sur les ignimbrites de Dschang (Ouest-Cameroun): Valorisation dans le bâtiment. Thèse Master of Science. Univ. Dschang (Cameroun), Fac. Sces, French; 2012.
24. Nesbitt HW, Young GM. Early Proterozoic climates and plate motions inferred from major element chemistry of luttites Nature. 1982; 291: 715–17.
25. Harnois L. The CIW index: A new chemical index of weathering. Sediment. Geol. 1988; 55: 319–22.

26. McDonough WF, Sun SS. Composition of the Earth. Chemical Geology. 1995;120(3-4): 223-53.
27. Gountié Dedzo M, Djamilatou Hamadjoda D, Fozing EM, Chako Tchamabé B, Ana Teresa Mendoza-Rosas AT, Asobo Nkengmatia EA et al. Petrology and geochemistry of ignimbrites and associated enclaves from Mount Bambouto, West-Cameroon, Cameroon Volcanic Line. Geochemistry. (In Press); 2020.
Acailable:https://doi.org/10.1016/j.chemer.2020.125663
28. Tchoua FM. Decouverte d'ignimbrites dans la région de Dschang (Cameroun). Ann. De la Fac des Sciences du Cameroun, French. 1968; 2:77-94.
29. Gountié Dedzo M. Séquence lithologique et étude du versant sud des Monts Bambouto. Mém. DEA. Univ. Yaoundé I, French; 2004.
30. Kwékam M, Hartmann G, Njanko T, Tcheumenak Kouémo J, Fozing EM, Njonfang E. Geochemical and Isotope Sr-Nd Character of Dschang Biotite Granite: Implications for the Pan-African Continental Crust Evolution in West-Cameroon (Central Africa). Earth Science Research. 2015; 24(1):88-102.
31. Bucher K, Grapes R. Petrogenesis of metamorphic rocks. Springer Science and Business Media; 2011.
32. Taylor SR, McLennan SM. The continental crust: Its composition and evolution: Oxford, Black well's; 1985.
33. Cullers RL. The chemical signature of source rocks in size fractions of Holocene stream sediment derived from metamophic rocks in the Wet Mountains region, Colorado, USA. Chemical Geology. 1994a; 113:327-43.
34. Cullers RL. The controls on the major and trace element variation of shales, siltstones, and sandstones of Pennsylvanian-Permian age from uplifted continental blocks in Colorado to platform sediment in Kansas, USA. Geochimica and Cosmochimica Acta. 1994b;58(22):4955-72.
35. Cullers RL, Graf JL. Rare Earth Elements in Igneous Rocks of the Continental Crust: Intermediate and Silicic Rocks-Ore Petrogenesis. In: Henderson, P., Ed., Rare Earth Element Geochemistry, Elsevier, Amsterdam; 1984.
36. Inoue A. Formation of clay minerals in hydrothermal environment. In: Velde, B. (Ed.), Origin and Mineralogy of Clays: Clays and the Environment. Springer, Berlin. 1995; 268–329.
37. Njoya A, Nkoumbou C, Grosbois C, Njopwouo D, Njoya D, Courtin NA, Yvon J, Martin F. Genesis of Mayouom kaolin deposit (West Cameroon). Applied Clay. Science. 2006; 32:125-40.
38. Meunier A, Velde B, Dudoignon P, Beaufort D. Identification of weathering and hydrothermal alteration in acidic rocks: Petrography and mineralogy of clay minerals. In: Pétrologie des altérations et des sols: Pétrologie des séquences naturelles. Colloque international du CNRS, Paris 4-7 juillet 1983. Strasbourg : Institut de Géologie – Université Louis-Pasteur. Sciences Géologiques. Mémoire, French. 1983; 2.
39. Dill HG, Bosse HR, Henning KH, Fricke A. Mineralogical and chemical variations in hypogene and supergene kaolin deposits in a mobile fold belt The Central Andes of northwestern Peru. Miner. Depos. 1997; 32:149–63.
40. Dill HG, Bosse HR, Kassbohm J. Mineralogical and chemical studies of volcanic-related argillaceous industrial minerals of the Central America Cordillera (Werstern Salvador). Econ. Geol. 2000; 95 (3):517–38.
41. Cassiaux M, Prout D, Shtari-Kauppi M, Sardini P, Leutsch Y. Clay minerals formed during propylitic alteration of a granite and their influence on primary porosity: A multi-scale approach. Clays and Clay Minerals. 2006; 54:541-54.
42. Ceryan S, Tudes S, Ceryan N. A new quantitative weathering classification for igneous rocks. Environmental Geology. 2008; 6:1319-36.
43. Yıldız A, Kuşcu M, Dumlupunar I, Krrem Aritan A, Begci M. The determination of the mineralogical alteration index and the investigation of the efficiency of the hydrothermal alteration on physic-mechanical properties in volcanic rocks from Koprulu, Afyonkarahisar, West Turkey. Bulletin of Engineering Geology and the Environment. 2010; 69:51-61.
44. Pola A, Crosta G, Fusi N, Barberini V, Norini G. Influence of alteration on physical properties of volcanic rocks. Tectonophysics. 2012; 566-567:67-86.

45. Braun JJ, Pagel M, Muller P, Bilong P, Michard A, and Guillet B. Cerium anomalies in lateritic profiles. Geochimica et Cosmochimica Acta. 1990; 54:781-95.
46. Sainsbury CL. Metallization and post-mineral hypogene argilization, Lost River tin mine alaska. Econ. Geol. 1960; 55:1478–1506.
47. Meyer C, Hemley JJ. Wall rock alteration. In: Barnes, H.L. (Ed.), Geochemistry of Hydrothermal Ore Deposits. New York, Holt, Rinehart, and Winston, Inc; 1967.
48. Eaton PC, Setterfield TN. The relationship between epithermal and porphyry hydrothermal systems within the Tavua Caldera, Fiji. Econ. Geol. 1993; 88: 1053–83.
49. Dill HG, Fricke A, Henning KH, Theune CH. Aluminium phosphate mineralization from the hypogene La Vanguardia kaolin deposit (Chile). Clay Miner. 1995b; 30:249–56.
50. Harvey CC. Exploration and assessment of kaolin clays formed from acid volcanic rocks on Coromandel Peninsula, North Island, New Zealand. Appl. Clay Sci. 1996; 11:381–92.
51. Hudson DM. Epithermal alteration and mineralization in the Comstock District, Nevada. Econ. Geol. 2003; 98: 367–85.
52. Soro Nibambin Siaka. Influence des ions fer sur les transformations thermiques de la
kaolinite. Thèse doctorat, Université de Limoges; French; 2003.
53. Charles N, Colin S, Gutierrez T, Lefebvre G. Mémento Kaolin et argiles kaoliniques. Rapport final. Rapport BRGM/RP-67334-FR, French; 2018.
54. Braun JJ, Viers J, Dupré B, Polve M, Ndam J, Muller JP. Solid/liquid REE fractionation in the lateritic system of Goyoum, East Cameroon: The implication for the present dynamics of soil covers of the humid tropical regions. Geochim. Cosmochim. Acta.1997; 62(2): 273– 99.
55. Nkalih MA. Cartographie et propriétés physicochimiques des argiles de Foumban (Ouest- Cameroun*)*. Thèse Doc. D'Etat, Univ. Yaoundé I, French; 2016.
56. Santos MC, Varajão AFDC, Yvon J. Genesis of clayey bodies in Quadrilàtero Ferrífero, Minas Gerais, Brazil. Catena .2004; 55:277–91.
57. Cases JM, Liétard O, Yvon J, Delon JF. Étude des propriétés cristallochimiques, morphologiques, superficielles de kaolinites désordonnées. Bull. Minéral. 1982; 105(5):439-55.
58. Petit S. Hétérogénéité et variabilité de la composition chimique des minéraux argileux : À quelle échelle ? Discussion de la notion de solution solide. HDR, Univ. Poitiers, France. French; 1994.
59. Esteoule-Choux J. Etude en microscopie électronique à balayage de quelques kaolins d'origines différentes : Apports de cette technique pour la compréhension de leur genèse. Clay Minerals, French. 1981; 16:279-88.
60. Weaver CE. The nature of TiO_2 in kaolinite. Clays and Clay Minerals. 1976; 24:215-18.
61. Tassongwa B, Nkoumbou C, Njoya D, Njoya A, Tchop JL, Yvon J et al. Geochemical and Mineralogical characteristics of the mayouom kaolin deposit, West Cameroon. Earth Science Research. 2014; 3(1):94-107.
62. Prudencio MI, Gouveia MA. REE distribution in present-day and ancient surface environments of Basaltic Rocks. Central Portugal. Clay Miner. 1995; 30: 239–48.
63. Cravero F, Dominguez E, Iglesias C. Genesis and applications of the Cerro Rubio kaolin deposit, Patagonia (Argentina). Appl. Clay Sci. 2001;18:157–72.
64. Nyakairu GWA, Koebrel C, Kurzweil H. The Buwambo kaolin deposit in central Uganda: Mineralogical and chemical composition. Chem. J. 2001; 35: 245–56.
65. Yusoff ZM, Ngwenyab BT, Parsons I. Mobility and fractionation of REEs during deep weathering of geochemically contrasting granites in a tropical setting, Malaysia. Chemical Geology. 2013;349–350:71–86.
66. Maulana A, Yonezu K, Watanabe K. Geochemistry of rare earth elements (REE) in the weathered crusts from the granitic rocks in Sulawesi Island, Indonesia. Journal of Earth Science. 2014; 25(3):460–72.
67. Danielson A, Möller P, Dulski P. The Europium anomalies in banded iron formations and the thermal history of the oceanic crust. Chemical Geology. 1992; 97:89-100.

68. Vidal P. Géochimie. Série géosciences. Dunod, Paris, French; 1998.
69. Bloundi Mohamed K. Etude géochimique de la lagune de Nador (Maroc oriental) : Impacts des facteurs anthropiques. *Thèse de doctorat Université Mohamed, Maroc.* 2005. French

Peer-review history:
The peer review history for this paper can be accessed here:
http://www.sdiarticle4.com/review-history/65528